Article

Discovery Medicine 2026; 38(206): 802–817
https://doi.org/10.24976/Discov.Med.202638206.66

SIRT3-mediated Deacetylation of IDH2 Reduces Mitochondrial Dysfunction and Improves Renal Ischemia-reperfusion Injury

Liang Xu[1,2], Bo Xu[2], Shijie Yao[3], Weijun Zhang[4], Xianghong Yang[1,2,*]

[1]Suzhou Medical College of Soochow University, 215123 Suzhou, Jiangsu, China
[2]Emergency and Critical Care Center, Intensive Care Unit, Zhejiang Provincial People's Hospital (Affiliated People's Hospital), Hangzhou Medical College, 310014 Hangzhou, Zhejiang, China
[3]Department of Nephrology, Zhong Da Hospital, Southeast University School of Medicine, 210009 Nanjing, Jiangsu, China
[4]Department of Neurology, The First Affiliated Hospital of Zhejiang Chinese Medical University (Zhejiang Provincial Hospital of Chinese Medicine), 310001 Hangzhou, Zhejiang, China
*Correspondence: yangxianghong@hmc.edu.cn (Xianghong Yang)
Submitted: 11 November 2025 Revised: 29 January 2026 Accepted: 27 February 2026 Published: 20 March 2026

Background: Renal ischemia-reperfusion injury (RIRI) is characterized by increased reactive oxygen species (ROS) and mitochondrial damage. Sirtuin 3 (SIRT3) promotes the deacetylation of isocitrate dehydrogenase 2 (IDH2) at lysine 413 (K413), thereby maintaining mitochondrial homeostasis. However, the roles of SIRT3 and IDH2 in RIRI remain unclear.
Methods: RIRI mouse models and hypoxia-reoxygenation (H/R)-exposed primary renal tubular epithelial cells (RTECs) were established, combined with adeno-associated virus and plasmid. Biochemical reagent kits, ELISA kits, hematoxylin and eosin staining, Transmission electron microscope, flow cytometry, Cell counting kit 8, co-immunoprecipitation and western blot assay were used. The role of SIRT3 overexpression in H/R-induced RTEC injury was investigated by plasmid transfection.
Results: Deacetylation of IDH2 (K413) ameliorated renal pathological damage and suppressed kidney injury indicators, malondialdehyde levels, and nicotinamide adenine dinucleotide (NAD) phosphate^{+}/NAD phosphate hydrogen ratio, while increasing superoxide dismutase activity, glutathione/glutathione disulfide ratio, NAD-IDH activity, and ATP levels ($p < 0.05$). It also reduced the proportion of damaged mitochondria and mitochondrial ROS. In H/R-induced RTEC cells, deacetylation of IDH2 (K413) also decreased mitochondrial function, ROS and oxidative stress levels ($p < 0.05$). Additionally, we confirmed an interaction between IDH2 and SIRT3, and observed that IDH2 acetylation levels significantly increased in RIRI and H/R models ($p < 0.01$). After deacetylation of IDH2 (K413) treatment, acetylated IDH2 (K413) ratio, the expression levels of oxidative phosphorylation enzymes (II, III, and V), cleaved caspase-3, and phosphorylated-dynamin-related protein 1 (Ser616) were decreased, while SIRT3 and phosphorylated-DRP1(Ser637) expression increased ($p < 0.05$). SIRT3 overexpression alleviated cell apoptosis, decreased mitochondrial ROS, and restored mitochondrial membrane potential ($p < 0.01$).
Conclusion: Overexpressing SIRT3 may alleviate RIRI by deacetylating IDH2, providing a theoretical basis for the pathogenesis research of RIRI.

Keywords: acute kidney injury; mitochondria; isocitrate dehydrogenase 2; acetylation; co-immunoprecipitation; transmission electron microscope

Introduction

Acute kidney injury (AKI) is characterized by a sudden decline in kidney function. Its incidence is relatively high in low- and middle-income countries, mainly due to acute illnesses, infection, and water pollution; in high-income countries, AKI predominantly occurs in critically ill patients and is associated with sepsis, hypotension, medication, or invasive surgery [1,2]. The global incidence of AKI among hospitalized patients is approximately 22% in adults and 34% in children [1]. The mortality rate of sepsis patients with AKI is as high as 32% [3,4], and approximately 20% of patients develop AKI due to ischemia-reperfusion injury caused by renal hilum clamping during surgery [5]. As a severe and life-threatening clinical condition, AKI is a major contributor to in-hospital mortality and imposes a substantial burden on healthcare systems. Renal ischemia-reperfusion injury (RIRI) is one of the main pathogenic factors of AKI. Recent research has shown that RIRI can induce increase production of in reactive oxygen species (ROS), mitochondrial damage, secretion of inflammatory factors, and microvascular dysfunction [6]. Exploring the underlying mechanisms of RIRI-induced AKI is beneficial for developing more effective therapeutic strategies.

Mitochondria are organelles widely present in eukaryotic cells, serving as the primary site of cellular respiration

and energy production. They not only produce adenosine triphosphate (ATP) via oxidative phosphorylation to supply energy for various cellular metabolism and maintain functional homeostasis, but also play key roles in regulating cellular metabolism, intracellular calcium homeostasis, cell signaling, apoptosis and other biological processes [7]. Recent studies indicate that mitochondrial dysfunction is crucial in the pathogenesis of AKI. Recent research found that mitochondrial ROS (mtROS) induces mitochondrial dysfunction and inflammation responses in AKI by disrupting mitochondrial DNA [8]. In AKI models, mitochondrial damage, especially in proximal renal tubular cells, is characterized by increased levels of reactive oxygen species (ROS), reduced ATP levels, and morphological changes, including swelling, cristae destruction, and loss of membrane integrity [9]. Significant mitochondrial damage and dysfunction have been observed in both AKI patients and animal models [10]. Agents targeting mitochondria have shown promising efficacy in preclinical trials [11]. However, there is still a lack of sufficient mechanism research on mitochondria as potential intervention targets in AKI, which limits the development of related pharmacological therapies.

Isocitrate dehydrogenase 2 (IDH2), a pivotal enzyme in the tricarboxylic acid (TCA) cycle and antioxidant pathway, localizes to mitochondria. It catalyzes isocitrate oxidative decarboxylation to produce α-ketoglutarate, thereby facilitating the biosynthesis of reduced nicotinamide adenine dinucleotide phosphate (NADPH) [12]. Silencing IDH2 attenuates TCA levels in cancer cells, suppresses ATP production, and inhibits glycolysis [13]. Accumulating evidence supports that overexpression of IDH2 can improve tissue damage in AKI mice [14]. Zheng *et al*. [15] reported that Sirtuin 5 overexpression alleviates liver injury in hepatic ischemia-reperfusion mice and promotes IDH2 expression. IDH2 overexpression enhances ATP production, mitochondrial membrane potential, and respiration in mouse proximal tubular S3 cells with hypoxia [16]. In mouse liver tissue, nicotinamide adenine dinucleotide (NAD^+) levels inversely correlate with IDH2 acetylation. NAD^+ is a key coenzyme in the mitochondrial electron transport chain, which suggests that IDH2 deacetylation may enhance mitochondrial respiratory function [17]. These findings support IDH2 deacetylation in mitigating tissue ischemia-reperfusion injury.

Sirtuin 3 (SIRT3), an evolutionarily conserved NAD^+-dependent deacetylase, belongs to the Sirtuin family and is primarily localized within mitochondria. It has been reported that renal tubular injury is related to stress-induced downregulation of SIRT3 and consequent mitochondrial dysfunction in proximal renal tubules [18]. SIRT3 exerts protective effects on alleviating RIRI via antioxidant stress [19]. Augmentation of SIRT3 levels can preserve mitochondrial integrity, significantly limit renal injury, and promote renal function recovery [20]. IDH2 is one of the target proteins of SIRT3 deacetylation [17]. SIRT3 deficiency results in an increased acetylation of IDH2 at lysine 413 (K413) [21]. Moreover, the deacetylation of IDH2 (K413) can be inhibited by SIRT3 knockdown [22]. Research revealed that mutant IDH2 exhibits K413 acetylation in cancer cells, which inhibits enzyme activity by reducing dimerization and blocking the binding of substrate (α-ketoglutarate) and cofactor (NADPH) [23]. It is unclear whether SIRT3 activation alleviates RIRI via IDH2. In short, reduced SIRT3 expression in AKI promotes acetylation of IDH2 at K413 and its enzyme activity, thereby contributing to mtROS accumulation and mitochondrial dysfunction. The specific underlying mechanisms warrant further exploration.

This study established a C57BL/6 mouse model *via* RIRI surgery. Additionally, an *in vitro* model of renal cell injury was established by exposing primary cultured renal tubular epithelial cells (RTECs) to a hypoxia-reoxygenation (H/R) environment. Using adeno-associated virus (AAV)-mediated transfection to mimic IDH2 deacetylation, the effects of IDH2 deacetylation on mitochondrial stabilization function and AKI amelioration were investigated at both animal and cellular levels. Furthermore, plasmid transfection was used to examine the role of SIRT3 overexpression in H/R-induced RTEC injury. This study aims to provide scientific evidence for elucidating underlying mechanisms and identifying potential therapeutic targets in the context of AKI.

Materials and Methods

Animal and Ethical Information

Forty-eight C57BL/6 mice (male, 7 weeks) were purchased from Shanghai SLAC Laboratory Animal Co., Ltd. (Shanghai, China). They were raised in Zhejiang Eyong Pharmaceutical Research and Development Center at 24 $\pm$ 2 °C, 55 $\pm$ 5% humidity, and a 12-h light/dark cycle, with no more than 6 mice housed in a single cage. All animal experiments were approved by Laboratory animal management and ethics committee of Zhejiang Provincial People's Hospital (Approval number: 20230715939350) and Animal Experimentation Ethics Committee of Zhejiang Eyong Pharmaceutical Research and Development Center (Approval number: ZJEY-20230724-01).

Intervention and Animal Grouping

After adaptive feeding for 5 days, 18 mice were divided into the sham and RIRI groups, 3 mice were randomly selected from each group for experiments at the 0-, 24-, and 72-h reperfusion time points (n = 3 for each group at each time point). This procedure was conducted to screen suitable reperfusion time and to make a preliminary observation of mitochondrial functional damage and protein expression. Furthermore, mice were injected with 50 µL (10^{11} viral genomes/100 µL) AAV2/9-

CMV-IDH2(K413R)-P2A-EGFP-3FLAG, AAV2/9-CMV-IDH2(K413Q)-P2A-EGFP-3FLAG, and AAV2/9-CMV-IDH2-P2A-EGFP-3FLAG (negative control, NC) via tail vein, to simulate deacetylation and acetylation of lysine, according to the study by Ma *et al*. [24]. AVV were designed and prepared by Genepharma (Jiangsu, China). Thirty mice were divided into five groups (6 mice per group): sham, RIRI, RIRI-NC, RIRI-IDH2_K413R, and RIRI-IDH2_K413Q, which aimed to explore the effects of IDH2 deacetylation. Animals were grouped using a random number table. Three randomly kidney tissues from each group were selected for HE staining, and TEM analysis, while the remaining 3 kidney tissues from the same group were used for flow cytometry and Western blot analysis.

Establishing Acute Kidney Injury Mice

Renal ischemic injury mouse models were established using renal ischemia-reperfusion injury (RIRI), according to the protocol described by Devarapu *et al*. [25]. RIRI was induced 3 weeks after AAV injection. In brief, mice were anesthetized using an isoflurane anesthesia machine (R546pro, RWD, Shenzhen, China), followed by disinfecting and preparing. Then, a 35-min unilateral renal pedicle clamping followed by 0-, 24-, or 72-h reperfusion was performed. The contralateral kidney was rapidly removed to prevent compensatory function, ensuring that the interval between the ischemic-side operation and the nephrectomy did not exceed 1 min. When the ischemic-side kidney gradually changed from bright red to dark red, it indicated successful ischemia. After 35 min of ischemia, the arterial clip was released, and reperfusion was confirmed by the kidney returning from dark red to bright red, suggesting restoration of renal blood flow. Then, the incision was sutured. After 0-, 24-, or 72-h reperfusion, mice were euthanized by CO_2 inhalation. During the experiment, mice experiencing $>$20% body weight loss would have been excluded and humanely euthanized. No mice were excluded from this study.

Detection of Biomarkers for Renal Injury, Renal Function, and Mitochondrial Dysfunction

After reperfusion for 0, 24, or 72 h, mice were anesthetized with isoflurane for cardiac blood collection and CO_2 euthanasia. Fresh kidneys were separated for fixation or cryopreservation. Serum creatinine (Scr) (220621201, Medicalsystem Biotechnology, China) and blood urea nitrogen (BUN) (220428101, Medicalsystem Biotechnology), renal function indicators, were detected using an automated biochemical instrument (Hitachi 3110, Hitachi, Tokyo, Japan). Renal injury biomarkers (serum KIM-1 and NGAL), renal oxidative stress indices (renal MDA, SOD, and GSH/GSSG), and renal mitochondrial function indices (renal $NADP^+$/NADPH, NAD-IDH, and ATP) were measured using a microplate reader (CMaxPlus, Molecular Devices, CA, USA). ELISA kits of KIM-1 (RX202640M), NGAL (RX202414M), SOD (RX021865M) and NAD-IDH assay kit (RXWB0431-96) were purchased from Ruixin Biotechnology Co., Ltd. (Quanzhou, China). Assay kits of GSH and GSSG (S0053) and $NADP^+$/NADPH (S0179) were purchased from Beyotime Biotechnology Co., Ltd. (Shanghai, China). Additionally, assay kits of MDA (A003-1-2) and ATP (A095-1-1) were purchased from Nanjing Jiancheng Bioengineering Institute (Nanjing, China). The above indicators were tested strictly according to the instructions of the manufacturers.

Hematoxylin and Eosin Staining

Hematoxylin and eosin (H&E) staining for pathological analysis of renal tissue was performed using staining kits of hematoxylin (H3136, Sigma-Aldrich, MA, USA) and eosin (E4009, Sigma-Aldrich). Briefly, mouse kidneys were fixed for 48 h, then embedded in paraffin. Paraffin sections of kidneys (3 µm) were dewaxed, rehydrated, and subjected to H&E staining. Finally, the sections were dehydrated with gradient ethanol, cleared in xylene, and sealed. Each section was detected in at least 5 fields of view.

Transmission Electron Microscope

A transmission electron microscope (TEM) was used to observe mitochondrial microstructure in renal tissue. Fresh kidneys were cut into 1 mm^3 cubes, and fixed using 2.5 % glutaraldehyde for 4 h. After washing and 1% osmic acid fixing for 2 h, samples were dehydrated and embedded in epoxy resin for TEM. Mitochondrial microstructure was observed and photographed using a JEM1400 TEM (JEOL, Akishima, Japan).

Cell Intervention and Grouping

Mouse primary renal tubular epithelial cells (RTECs) (MIC-iCell-u001) were cultured in specialized culture system (PriMed-iCell-001) (complete medium). RTECs and complete medium were purchased from iCell Bioscience Inc. (Shanghai, China). Cells were routinely tested negative for mycoplasma contamination. According to He *et al*. [26], the hypoxic environment consisted of 1% O_2, 5% CO_2 and 94% N_2, and reoxygenation environment was performed under 5% CO_2 and 95% air. RTECs (3 passages) at 2×10^6 cells were seeded into T25. After one day, RTEC were cultured in serum-free DMEM/F12 without glucose for 12 h under hypoxic conditions, followed by reoxygenation for 0–48 h. Cells were divided into the Control and H/R groups.

Additionally, according to previous reports [24], cells were incubated with AAV2/9-CMV-IDH2(K413R)-P2A-EGFP-3FLAG, AAV2/9-CMV-IDH2(K413Q)-P2A-EGFP-3FLAG, AAV2/9-CMV-IDH2-P2A-EGFP-3FLAG (NC) for 16 h. Subsequently, the RTECs underwent 12-h hypoxic treatment with 24-h reoxygenation and were divided into five groups: Control, H/R, H/R-NC,

H/R+IDH2_K413R, H/R+IDH2_K413Q, to explore the effects of deacetylation and acetylation on mitochondrial dysfunction. Moreover, RTECs were transfected with either a control plasmid vector (NC) or a plasmid carrying SIRT3 cDNA (sequence information provided in **Supplementary File 1**) using Lipofectamine 2000 (11668019, Invitrogen, CA, USA) for 48 h according to He *et al.* [26], followed by H/R treatment. Subsequently, RTECs were divided into four groups: Control, H/R, H/R+OE-SIRT3, H/R+OE-NC, to explore SIRT3's effects on mitochondrial dysfunction. RTEC images were captured under the bright field using an optical microscope (AE200, Motic, Xiamen, China).

Detection of Mitochondrial ROS and Membrane Potential

Mitochondrial ROS (mtROS) and membrane potential (MMP) were used to evaluate the degree of mitochondrial dysfunction in renal tissues and RTECs. Renal tissues were minced and digested. After washing, the tissues were prepared as a single cell suspension. For mtROS detecting, cells (2×10^7 cells/mL) were incubated with a mitoSOX green fluorescence probe (M36005, Invitrogen, USA) for 15 min. For MMP detecting, RTEC suspension (2×10^6/mL) was incubated with JC-1 fluorescence probe (C2006, Beyotime) for 20 min. After washing, centrifugation, and resuspension, mean fluorescence intensity (MFI) was detected using a NovoCyte 2000 flow cytometer with NovoExpress software (Version 1.6.2; Agilent Technologies, CA, USA).

Cell Viability Assay

Cell counting kit 8 (CCK8) (C0039, Beyotime, China) was used for cell viability assay. Briefly, 100 µL cells (1×10^5 cells/mL) were seeded on 96-well plates. After 12-h hypoxic and 24-h reoxygenation, CCK8 reagents were mixed with complete medium (1:100) and used to incubate cells for 4 h. A microplate reader was used to detect optical density values at 450 nm.

Cell Apoptosis Detection

RTEC apoptosis was detected using an Annexin V-FITC /PI kit (556547, BD biosciences, NJ, USA) and flow cytometry (NovoCyte, Agilent). After washing, RTECs (1×10^6 cells/mL) were incubated with Annexin V-FITC and PI for 15 min in the dark. Finally, positive cell proportion was detected using a flow cytometry.

Co-immunoprecipitation and Western Blot Assay

Co-immunoprecipitation (Co-IP) and western blot (WB) were performed to observe the acetylation levels of IDH2 and its interaction with STIR3 in renal tissue and cells. Total protein was extracted from tissue homogenate or cells using IP lysis buffer (P0013J, Beyotime, China) supplemented 1% deacetylase inhibitor mixture (P1112, Beyotime) and protease and phosphatase inhibitor (P1045, Beyotime), The lysates were then incubated with either rabbit IgG (1:200, ab46540, Abcam, UK) or IDH2 antibody (1:200, 82117-1-RR, Proteintech, China) at 4 °C for 2 h. Then, protein A/G agarose beads were added for 12-h incubation. Subsequently, the IP complexes were washed and subjected to WB analysis. After adding loading buffer (P0015N-2ml, Beyotime, China), total protein or IP complexes were boiled for 5 min. Then, the samples were separated by electrophoresis and transferred onto PVDF membranes (10600023, GE Healthcare Life, MA, USA). Membranes were incubated with specific antibodies (Table 1). Briefly, after incubation with a developer, the signals were captured using a chemiluminescence analyzer (610020-9Q, Qinxiang, Shanghai, China), and the relative grayscale values of protein bands were quantified using ImageJ (Version 1.51j8; National Institutes of Health, MD, USA).

Statistical Analysis

IBM SPSS Statistics (Version 20.0; IBM Corp., NY, USA) was used for statistical analysis. All experiments were repeated at least 3 times. For normally distributed data, the independent-samples *t*-test was applied to compare the differences between two groups. Comparisons among multiple groups were performed using one-way ANOVA followed by Tukey's post-hoc or Dunnett's T3 tests, as appropriate. The Kruskal-Wallis H test was used to analyze non-normally distributed data. Results were presented as mean ± standard deviation (SD). A *p*-value less than 0.05 was considered statistically significant. All statistical processes followed the double-blinded principle.

Results

Renal Ischemia-reperfusion Leads to Renal Tissue and Functional Damage and Mitochondrial Dysfunction With Increased Levels of Oxidative Stress, mtROS, and Acetylated IDH2

This study established a renal ischemic injury model using 35-min unilateral renal pedicle clamping followed by 0-, 24-, or 72-h reperfusion, as described by Devarapu *et al.* [25]. Renal histopathological changes were assessed by H&E staining. In RIRI mice with 1-day reperfusion, renal tissue was severely damaged with many renal tubules vacuolized and glomeruli atrophied. Interestingly, tissue damage in mice after 72 h of reperfusion was reduced compared to that observed at 24 h (Fig. 1A). Consistent with the pathological results, there was a significant increase in indicators of renal function in RIRI mice with 24 and 72-h reperfusion, including increased levels of BUN, Scr, KIM-1, and NGAL ($p < 0.05$) (Fig. 1B,C). Furthermore, markers of oxidative stress (MDA, SOD, and GSH/GSSG) and mitochondrial function ($NADP^+$/NADPH, NAD-IDH, and ATP) are detected using different assay kits. The levels of MDA and $NADP^+$/NADPH increased in RIRI mice with 24-/72-h reperfusion ($p < 0.05$), while levels of SOD,

Table 1. Western blot antibody information.

Antibody	Company	Cat#	Dilution ratio
Anti-IDH2 antibody	Proteintech	82117-1-RR	1:10000
Anti-Ac-IDH2(K413) antibody	GeneTel Laboratories LLC	AC0004	1:10000
Anti-SIRT3 antibody	Abcam	ab246522	1:10000
Anti-Cleaved Caspase-3 antibody	Abcam	ab214430	1:10000
Total OXPHOS Rodent WB Antibody	Abcam	ab110413	1:10000
Anti-DRP1 antibody [EPR19274]	Abcam	ab184247	1:10000
Phospho-DRP1 (Ser637) Antibody	Affinity	DF2980	1:10000
Anti-DRP1 (phospho S616) antibody	Affinity	AF8470	1:10000
Anti-rabbit IgG, HRP-linked Antibody	CST	7074	1:10000
Goat Anti-Mouse IgM Antibody	CST	46315	1:10000
GAPDH Antibody	Proteintech	10494-1-AP	1:10000

IDH2, isocitrate dehydrogenase 2; K413, lysine 413; SIRT3, Sirtuin 3; DRP1, dynamin-related protein 1; GAPDH, glyceraldehyde-3-phosphate dehydrogenase; OXPHOS, oxidative phosphorylation.

GSH/GSSG, NAD-IDH, and ATP decreased ($p < 0.01$) (Fig. 1B,C). Moreover, mtROS were measured using a mitoSOX green (MSG) fluorescence probe and flow cytometry. The MFI of mtROS in RIRI mice with 24-/72-h reperfusion increased to over 150% that in sham mice ($p < 0.01$) (Fig. 1D).

Due to the significant acute kidney injury can be observed after 24-h reperfusion, 24-h reperfusion was chosen for subsequent experiments. Co-IP was performed to observe the acetylation levels of IDH2 and its interaction with STIR3 in RIRI mice with 24-h reperfusion. The levels of acetylated protein and K413 acetylation of IDH2 protein increased in the renal tissues of RIRI mice ($p < 0.05$) (Fig. 1E,F). SIRT3 proteins existed in the precipitation complex of IDH2 protein and decreased in RIRI mice with 24-h reperfusion compared to sham mice ($p < 0.01$) (Fig. 1E,F).

Deacetylation of IDH2 Alleviates Renal Tissue Damage and Mitochondrial Dysfunction

Given that the acetylation level of IDH2, particularly at lysine 413 (K413), was upregulated in the renal tissue of RIRI mice, this study simulated deacetylation by mutating K413 to arginine (R) and acetylation by mutating K413 to glutamine (Q) in RIRI mice subjected to 24-h reperfusion. RIRI mice exhibited significant pathological damage, including many renal tubules vacuolized and glomeruli atrophied (Fig. 2A). Correspondingly, renal function indicators BUN, Scr, KIM-1, and NGAL have increased in RIRI mice compared to sham mice ($p < 0.01$) (Fig. 2B,C). As expected, mutating K to R partially reversed the pathological damage and levels of renal function indicators in RIRI-NC mice ($p < 0.05$) (Fig. 2B,C). Mice treated with simulated acetylation (K413Q) exhibited pathological damage and renal function indicator levels in the kidney similar to those in the RIRI mouse group (Fig. 2A–C) (RIRI-NC vs. RIRI-IDH2_K413Q: BUN $p = 0.225$, Scr $p = 0.844$, KIM-1 $p = 0.542$, NGAL $p = 0.789$).

Additionally, the increased MDA and $NADP^+$/NADPH levels in RIRI-NC mice were reduced by mutating K to R ($p < 0.05$) (Fig. 2D). Meanwhile, decreased SOD, GSH/GSSG, NAD-IDH, and ATP were observed in RIRI mice compared to sham mice. Furthermore, mutation of K to R partially reversed these parameters compared to RIRI-NC mice ($p < 0.05$) (Fig. 2D). There were no significant differences in the simulated acetylation (K413Q) group compared to RIRI-NC (RIRI-NC vs. RIRI-IDH2_K413Q: MDA $p = 0.268$, SOD $p = 0.45$, GSH/GSSG $p = 0.099$, $NADP^+$/NADPH $p = 0.781$, NAD-IDH $p = 0.515$, ATP $p = 0.483$).

Deacetylation of IDH2 Improves Mitochondrial Ultrastructure and Reduces mtROS Level in the Renal Tissue of RIRI Mice

This study used TEM to observe mitochondrial microstructure in renal tissue. Compared to sham mice, more mitochondria exhibited mitochondrial swelling and spine rupture (Fig. 3A). Additionally, mutating K to R decreased mitochondria with microstructural damage in RIRI mice (Fig. 3A). Furthermore, the MFI of mtROS in RIRI mice increased in sham mice ($p < 0.01$) (Fig. 3B,C), meanwhile, mutating K to R markedly decreased it in RIRI mice ($p < 0.05$) (Fig. 3B,C).

Additionally, the levels of K413 acetylation of IDH2, cleaved caspase-3, OXPHOS complex II (CII), complex III (CIII), complex V (CV), and p-DRP1 (Ser616) protein increased in RIRI mice compared to sham mice ($p < 0.01$), whereas SIRT3 and p-DRP1 (Ser637)/DRP1 decreased ($p < 0.01$). The levels of K413 acetylation of IDH2, cleaved caspase-3, CII, CIII, CV, and p-DRP1 (Ser616) protein were decreased in RIRI mice with the mutation of K to R of IDH2_K413 ($p < 0.05$) (Fig. 3D,E). There were no significant differences in the simulated acetylation (K413Q) group compared to RIRI-NC (Fig. 3A–E) (RIRI-NC vs. RIRI-IDH2_K413Q: MFI of mtROS $p = 0.153$, Ac-IDH2(K413)/IDH2 $p = 0.114$, SIRT3/GAPDH

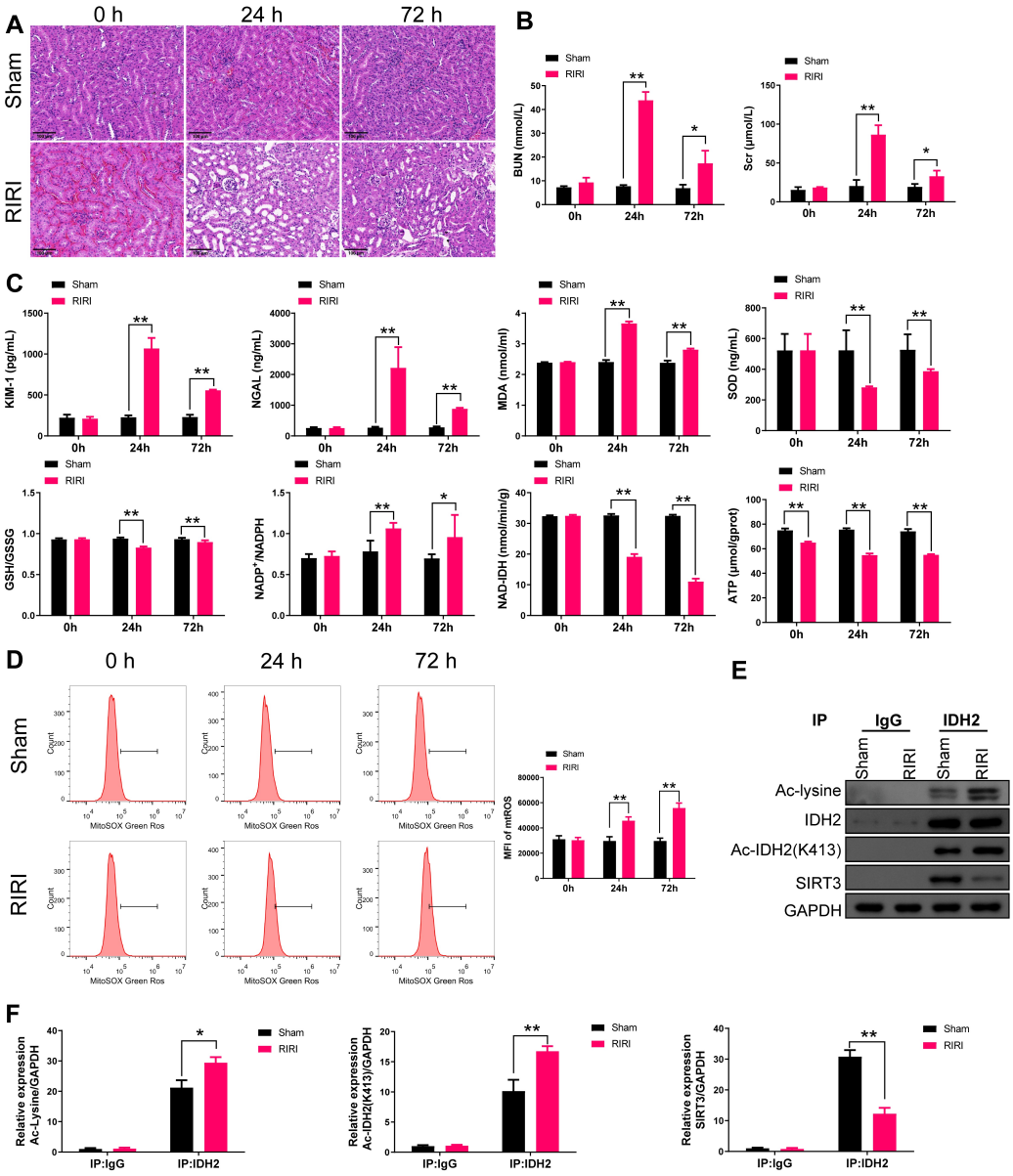

Fig. 1. Renal ischemia-reperfusion leads to renal tissue and functional damage and mitochondrial dysfunction with increased levels of oxidative stress, mtROS, and acetylated IDH2. RIRI mice were established using 35-min unilateral renal pedicle clamping followed by 0-, 24-, or 72-h reperfusion. (A) H&E staining for pathological damage to renal tissue showed that 24- or 72-h reperfusion induced pathological damage ($n = 3$). (B) Scr and BUN were detected using an automated biochemical instrument ($n = 3$). They were increased in RIRI mice with 24- or 72-h reperfusion. (C) Renal injury biomarkers (serum KIM-1 and NGAL), renal oxidative stress indices (MDA, SOD, and GSH/GSSG), and mitochondrial function indices ($NADP^+$/NADPH, NAD-IDH, and ATP) were measured using a microplate reader. KIM-1, NGAL, MDA, and $NADP^+$/NADPH increased after 4- or 72-h reperfusion, while others decreased ($n = 3$). (D) MtROS were measured using a mitoSOX green fluorescence probe and flow cytometry; the values on the line segment represent the proportion of cells with mtROS-positive; MFI of mtROS is the average mtROS content per mtROS-positive cell in mROS-positive cells. It was increased in the renal tissue of RIRI mice ($n = 3$). (E,F) Co-IP was used to observe the acetylation levels of IDH2 and its interaction with STIR3 in RIRI mice with 24-h reperfusion ($n = 3$). Mean ± SD, $*p < 0.05$, $**p < 0.01$, *vs.* Sham group. List of abbreviations: RIRI, Renal ischemia-reperfusion injury; mtROS, mitochondrial reactive oxygen species; $NADP^+$, nicotinamide adenine dinucleotide phosphate; NADPH, nicotinamide adenine dinucleotide phosphate hydrogen; IDH2, isocitrate dehydrogenase (NADP(+)) 2; H&E, hematoxylin and eosin; Scr, serum creatinine; BUN, blood urea nitrogen; KIM-1, kidney injury molecule-1; NGAL, neutrophil gelatinase-associated lipocalin; MDA, malondialdehyde; SOD, superoxide dismutase; GSH, Glutathione; GSSG, glutathione disulfide; NAD-IDH, Nicotinamide adenine dinucleotide-dependent isocitrate dehydrogenase; ATP, adenosine triphosphate; mitoSOX, mitochondrial superoxide; MFI, mean fluorescence intensity; Co-IP, co-immunoprecipitation.

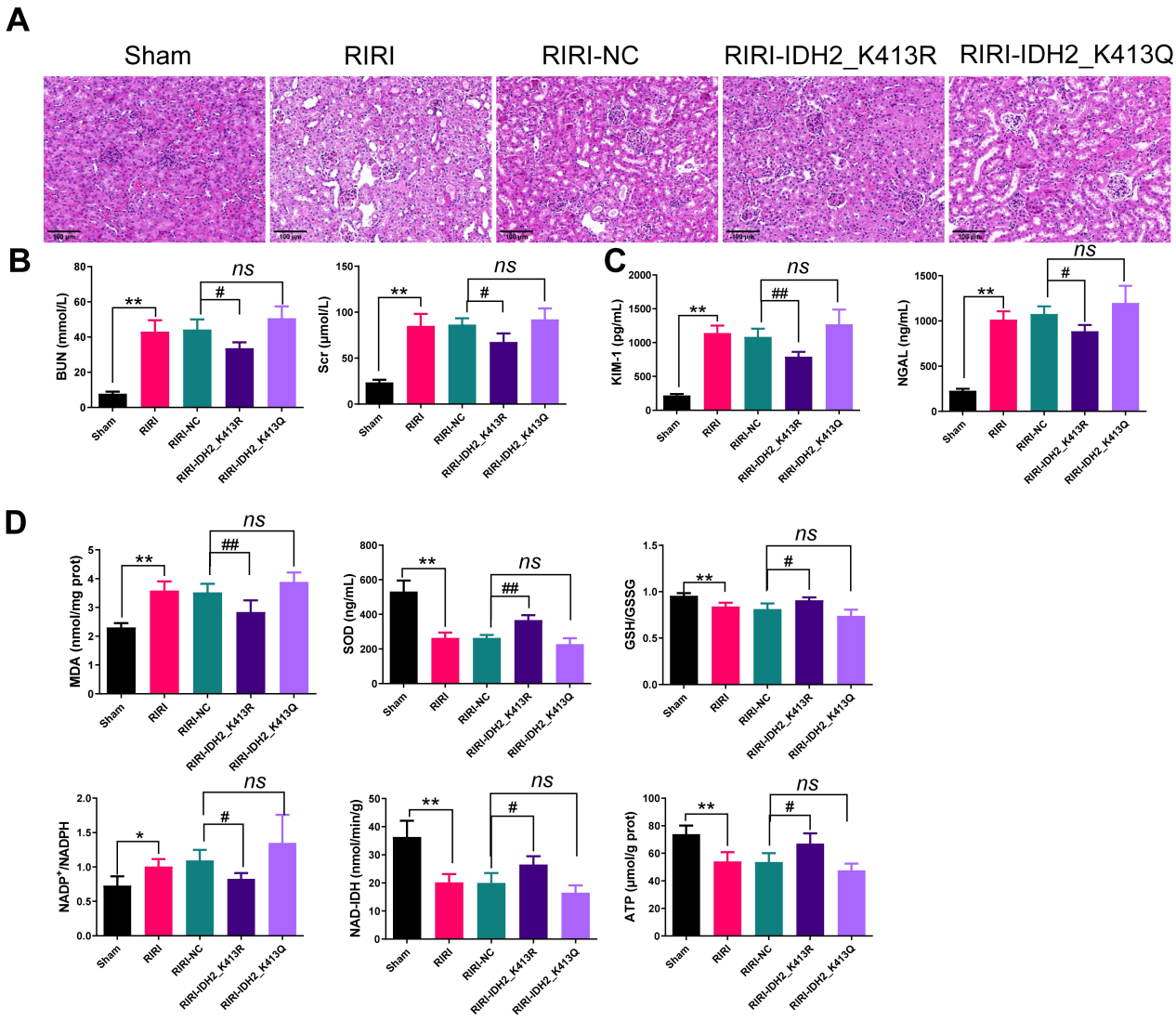

Fig. 2. Deacetylation of IDH2 alleviates renal tissue damage and mitochondrial dysfunction. Directional mutation of IDH2 acetylation site (K413) was performed by tail vein injection of adeno-associated virus. After 3 weeks, RIRI mice were established using 35-min unilateral renal pedicle clamping followed by 0-, 24-, or 72-h reperfusion. (A) H&E staining for pathological damage to renal tissue showed that mutating K to R (K413R) at 413-site improved pathological damage ($n = 3$). (B) Scr and BUN were detected using an automated biochemical instrument ($n = 6$). After mutating K to R (K413R), they decreased in RIRI mice with 24-h reperfusion. (C) Renal injury biomarkers (serum KIM-1 and NGAL) were measured using a microplate reader ($n = 6$) and were decreased after mutating K to R (K413R). (D) Renal oxidative stress indices (MDA, SOD, and GSH/GSSG), and mitochondrial function indices ($NADP^+$/NADPH, NAD-IDH, and ATP) were measured using a microplate reader ($n = 6$). Mean ± SD, $*p < 0.05$, $**p < 0.01$, *vs.* Sham group; $^{ns}p > 0.05$, $\#p < 0.05$, $\#\#p < 0.01$, *vs.* RIRI-NC group. List of abbreviations: K, lysine; R, arginine; RIRI, Renal ischemia-reperfusion injury; $NADP^+$, nicotinamide adenine dinucleotide phosphate; NADPH, nicotinamide adenine dinucleotide phosphate hydrogen; IDH2, isocitrate dehydrogenase (NADP(+)) 2; H&E, hematoxylin and eosin; Scr, serum creatinine; BUN, blood urea nitrogen; KIM-1, kidney injury molecule-1; NGAL, neutrophil gelatinase-associated lipocalin; MDA, malondialdehyde; SOD, superoxide dismutase; GSH, Glutathione; GSSG, glutathione disulfide; NAD-IDH, Nicotinamide adenine dinucleotide-dependent isocitrate dehydrogenase; ATP, adenosine triphosphate.

$p = 0.248$, cleaved caspase 3/GAPDH $p = 0.258$, OXPHOS complex I (CI)/GAPDH $p = 1.000$, CII/GAPDH $p = 0.621$, CIII/GAPDH $p = 0.077$, OXPHOS complex IV (CIV)/GAPDH $p = 0.993$, CV/GAPDH $p = 0.426$, p-Drp1(Ser637)/Drp1 $p = 0.987$, p-Drp1(Ser616)/Drp1 $p = 0.472$).

H/R Inhibits Viability and Promotes Cell Apoptosis, Oxidative Stress, and Mitochondrial Dysfunction in Primary RTECs

To clarify the potential mechanism, this study primarily cultured RTECs in a 12-h hypoxia environment, followed by 0-48-h reoxygenation, and decreased cell den-

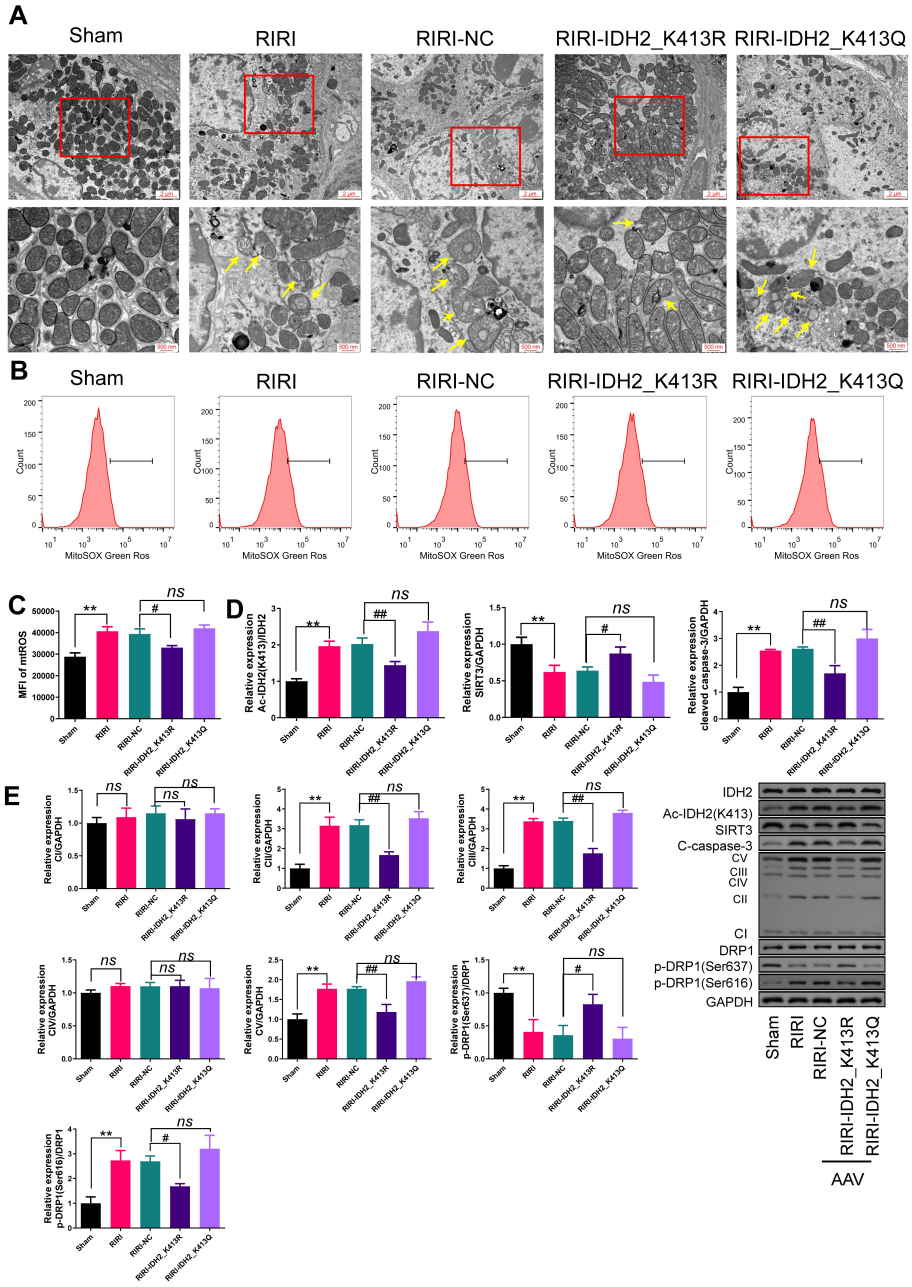

Fig. 3. Deacetylation of IDH2 improves mitochondrial ultrastructure and reduces mtROS level in renal tissue of RIRI mice. Directional mutation of IDH2 acetylation site (K413) were performed by tail vein injection of adeno-associated virus. After 3 weeks, RIRI mice were established using 35-min unilateral renal pedicle clamping followed by 0-, 24-, or 72-h reperfusion. (A) A transmission electron microscope was used to observe mitochondrial ultrastructure (n = 3). Mutating K to R (K413R) at 413-site improved the destruction of mitochondrial structure in RIRI mice. (B,C) MtROS were measured using a mitoSOX green fluorescence probe and flow cytometry; MFI of mtROS is the average mtROS content per mtROS-positive cell in mtROS-positive cells. MtROS decreased in the renal tissue of RIRI mice with the mutation of K to R (K413R) (n = 3). (D,E) Western blot assay was used to detect protein expression in the renal tissue of RIRI mice. IDH2 acetylation (K413)/IDH2, cleaved caspase-3, OXPHOS complex II/III/V (CII/CIII/CV), p-DRP1 (Ser616)/DRP1 levels decreased in the renal tissue of RIRI mice with mutation of K to R (K413R), while SIRT3 and p-DRP1 (Ser637)/DRP1 decreased. There was no significant change in OXPHOS complex I/IV (CI/CIV) expression (n = 3). Mean ± SD, $^{**}p < 0.01$, *vs.* Sham group; $^{ns}p > 0.05$, $\#p < 0.05$, $\#\#p < 0.01$, *vs.* RIRI-NC group. List of abbreviations: IDH2, isocitrate dehydrogenase (NADP(+)) 2; mtROS, mitochondrial reactive oxygen species; RIRI, Renal ischemia-reperfusion injury; K, lysine; R, arginine; mitoSOX, mitochondrial superoxide; C-caspase-3, cleaved caspase-3; MFI, mean fluorescence intensity; OXPHOS, oxidative phosphorylation; DRP1, dynamin-related protein 1; p-DRP1, phosphorylated DRP1; Ser, serine; GAPDH, glyceraldehyde-3-phosphate dehydrogenase.

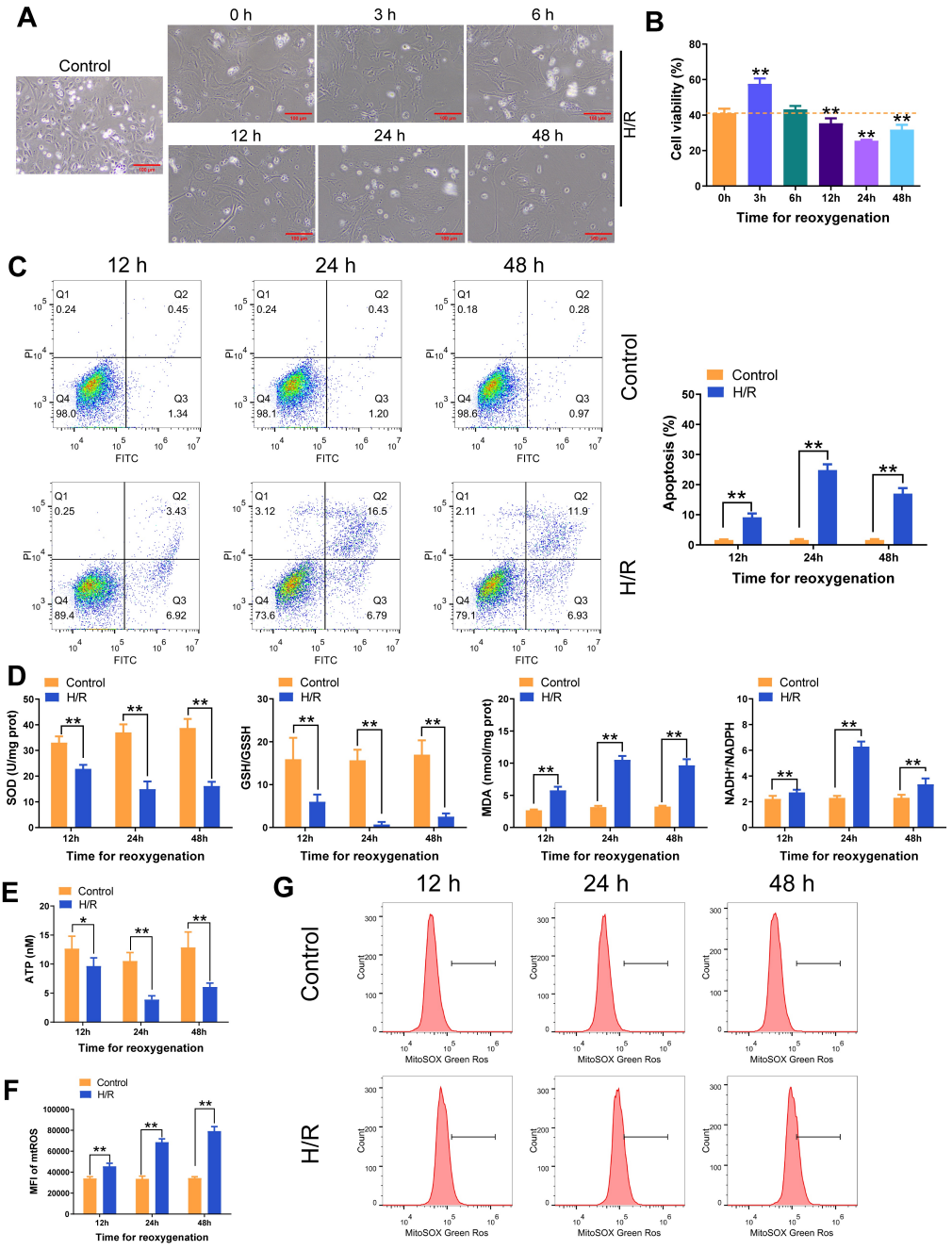

Fig. 4. H/R inhibits viability and promotes cell apoptosis, oxidative stress, and mitochondrial dysfunction in primary RTECs. Primarily RTECs were cultured in a 12-h hypoxia environment, followed by 0-48-h reoxygenation. (A) RTEC images were captured under the bright field using an optical microscope (200×, 100 μm). (B) Cell counting kit 8 was used for cell viability detection. Reoxygenation for 12/24/48-h decreased RTEC viability (**$p < 0.01$ *vs.* 0h group). (C) Annexin V-FITC/PI kit and flow cytometry were used to detect apoptosis. Reoxygenation for 12/24/48-h increased RTEC apoptosis. (D,E) RTEC oxidative stress indices (MDA, SOD, and GSH/GSSG) and mitochondrial function indices ($NADP^+$/NADPH and ATP) were measured using a microplate reader. Reoxygenation for 12/24/48 h increased MDA and $NADP^+$/NADPH and decreased SOD, GSH/GSSH, and ATP. (F,G) MtROS were measured using a mitoSOX green fluorescence probe and flow cytometry; MFI of mtROS is the average mtROS content per mtROS-positive cell in mtROS-positive cells. MtROS increased in H/R-exposed RTECs with 12/24/48-h reoxygenation. Mean ± SD, $n = 3$. *$p < 0.05$, **$p < 0.01$, *vs.* Control group. List of abbreviations: H/R, hypoxia/reoxygenation; RTECs, renal tubular epithelial cells; MDA, malondialdehyde; SOD, superoxide dismutase; GSH, glutathione; GSSG, glutathione disulfide; $NADP^+$, nicotinamide adenine dinucleotide phosphate; NADPH, nicotinamide adenine dinucleotide phosphate hydrogen; ATP, adenosine triphosphate; mtROS, mitochondrial reactive oxygen species; MFI, mean fluorescence intensity.

sity was observed under an optical microscope (Fig. 4A). CCK8 was used for cell viability detection. After 12/24/48-h reoxygenation, cell viability of RTECs significantly decreased, while it increased after 3-h reoxygenation ($p < 0.01$) (Fig. 4B). Flow cytometry detection showed that cell apoptosis was increased after 12/24/48-h reoxygenation ($p < 0.01$) (Fig. 4C). As expected, SOD, GSH/GSSH, and ATP levels decreased in 12-h hypoxic RTECs subjected to 12/24/48-h reoxygenation ($p < 0.05$), while MDA and $NADP^+$/NADPH increased ($p < 0.01$) (Fig. 4D,E). Furthermore, the MFI of mtROS in these 12-h hypoxic RTECs hugely increased compared to their controls ($p < 0.01$) (Fig. 4F,G).

Furthermore, IDH2 activity was significantly suppressed after 12-h hypoxia/12/24/48-h reoxygenation ($p < 0.05$) (Fig. 5A), while IDH2 acetylation (K413) and CII/III/V increased ($p < 0.01$) (Fig. 5B,C). Additionally, Co-IP was performed to observe the acetylation levels of IDH2 and its interaction with STIR3. The levels of acetylated protein and K413 acetylation of IDH2 protein increased in 24-h reoxygenation RTECs ($p < 0.05$) (Fig. 5D). SIRT3 proteins existed in the precipitation complex of IDH2 protein and decreased in RIRI mice with 24-h reperfusion compared to control mice ($p < 0.01$) (Fig. 5D).

Deacetylation of IDH2 Suppresses Oxidative Stress and mtROS Levels in Primary RTECs With H/R and Improves Mitochondrial Dysfunction

Considering that 24-h reoxygenation induced the highest level of cell apoptosis, this time point was selected for intervention in IDH2 mutant cells. As expected, cell viability and levels of SOD, GSH/GSSH, and APT were markedly decreased in group H/R; compared to group H/R-NC, they increased in group H/R+IDH2_K413R ($p < 0.05$) (Fig. 6A,B). Additionally, mutating K to R suppressed MDA and $NADP^+$/NADPH levels in H/R-exposed RTECs ($p < 0.05$) (Fig. 6B). Furthermore, apoptotic and the MFI of mtROS in H/R-exposed RTECs increased ($p < 0.01$), while mutating K to R reversed them ($p < 0.01$) (Fig. 6C,D). Additionally, JC-1 staining was used to membrane potential (MMP). The MMP is directly proportional to the expression level of JC-1 aggregates. Relative fluorescence intensity of JC-1 aggregates decreased in H/R RTECs compared to the control, while mutating K to R increased it compared to H/R-NC RTECs ($p < 0.01$) (Fig. 6E), indicating mitochondrial dysfunction. However, there were no significant differences in the simulated acetylation (K413Q) group compared to RIRI-NC (Fig. 6A–E) (H/R-NC vs. H/R-IDH2_K413Q: cell viability in Fig. 6A $p = 0.071$; in Fig. 6B SOD $p = 0.492$, MDA $p = 0.502$, GSH/GSSH $p = 0.423$, $NADP^+$/NADPH $p = 0.515$, ATP $p = 0.763$; apoptotic in Fig. 6C $p = 0.154$; MFI of mtROS in Fig. 6D $p = 1$; JC-1 aggregates in Fig. 6E $p = 0.222$).

Furthermore, IDH2 activity and expression levels of SIRT3 and p-DRP1(Ser637) protein decreased in H/R RTECs, while cleaved caspase-3, IDH2 acetylation (K413)/IDH2, CII/III/V and p-DRP1(Ser616) significantly increased ($p < 0.01$) (Fig. 6F–I). Mutating K to R reversed these changes ($p < 0.05$) (Fig. 6F–I), whereas mutation of K to Q showed no significant difference compared to the RIRI-NC group (Fig. 6F–I) (H/R-NC vs. H/R-IDH2_K413Q: IDH2 in Fig. 6F $p = 0.59$; in Fig. 6G Ac-IDH2(K413)/IDH2 $p = 0.777$, SIRT3/GAPDH $p = 0.447$, cleaved caspase 3/GAPDH $p = 0.927$, CI/GAPDH $p = 0.999$, CII/GAPDH $p = 0.835$, CIII/GAPDH $p = 0.600$, CIV/GAPDH $p = 0.994$, CV/GAPDH $p = 0.745$, p-Drp1(Ser637)/Drp1 $p = 0.756$, p-Drp1(Ser616)/Drp1 $p = 0.249$).

Overexpression of SIRT3 Inhibits Apoptosis and mtROS, While Improving Mitochondrial Dysfunction and Decreasing IDH2 Acetylation (K413) of H/R-exposed RTECs

Transfection efficiency of SIRT3 overexpression is 86.28 ± 2.82%, compared with 82.46 ± 9.55 for its control (OE-NC) (**Supplementary Fig. 1**). SIRT3 overexpression in RTECs was used to explore SIRT3's effects on IDH2 and mitochondrial function. In H/R-exposed RTECs, SIRT3 overexpression inhibited the apoptosis and mtROS compared to the controls ($p < 0.01$) (Fig. 7A,B). In addition, after overexpressing SIRT3, the relative fluorescence intensity of JC-1 aggregates was increased in H/R-exposed RTECs ($p < 0.01$) (Fig. 7C), while ATP level and IDH2 activity were increased ($p < 0.01$) (Fig. 7D). WB assay results showed that overexpressing SIRT3 decreased IDH2 acetylation (K413)/IDH2 level and increased SIRT3 expression in H/R-exposed RTECs (Fig. 7E,F).

Discussion

RIRI typically induces pathological damage in renal tissue, mainly manifesting as tubular dilation, necrosis, and fibrosis. Godoy *et al.* [27] showed that 24-h reperfusion induced the most pronounced tubular injury in RIRI mouse models, with obvious tubular dilation. Consistent with prior findings, reperfusion duration correlated with AKI severity, and 24-hour reperfusion caused more substantial renal tissue injury. BUN and Scr are conventional clinical markers of kidney injury. Meanwhile, KIM-1 and NGAL represent emerging biomarkers of kidney injury [28]. We observed that kidney injury indicators were higher than those in the control group at both 24-h and 72-h of reperfusion, which was in line with histopathological findings. Moreover, these indicators in RIRI mice with 24-h reperfusion were higher than those in RIRI mice with 72-h reperfusion. Our study highlights that 24-h reperfusion induced more severe renal injury, rendering it more appropriate for establishing RIRI mouse models.

Maintaining mitochondrial homeostasis delays chronic kidney disease progression. Mitochondria serve as

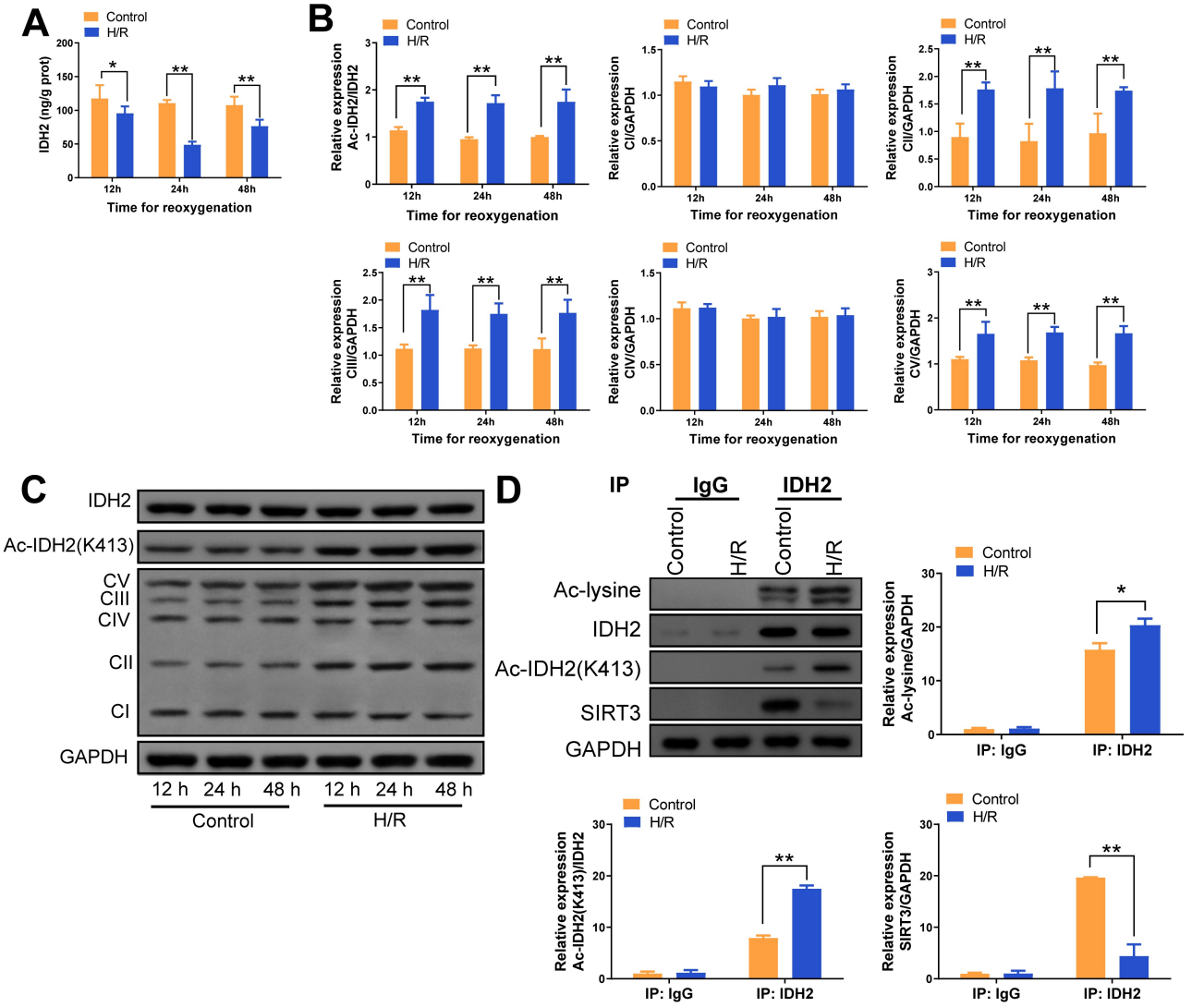

Fig. 5. Reoxygenation for 12/24/48-h decreased IDH2 and increased IDH2 acetylation (K413), OXPHOS complex II/III, and OXPHOS complex V expression of H/R-exposed RTECs. Primarily, RTECs were cultured in a 12-h hypoxia environment followed by 0-48-h reoxygenation. (A) IDH2 content was detected using ELISA. Reoxygenation for 12/24/48-h decreased it. (B) Western blot assay was used to detect protein expression in RTECs. IDH2 acetylation (K413)/IDH2, cleaved caspase-3, OXPHOS complex II/III/V (CII/CIII/CV) levels increased in RTECs with 12/24/48-h reoxygenation. There was no significant change in OXPHOS complex I/IV (CI/CIV) expression. (C) Representative images of protein bands. (D) Co-IP was used to observe the acetylation levels of IDH2 and its interaction with STIR3 in RTECs with 12-h hypoxia and 24-h reoxygenation ($n = 3$). Mean ± SD, $n = 3$. *$p < 0.05$, **$p < 0.01$, *vs.* Control group. List of abbreviations: H/R, hypoxia/reoxygenation; RTECs, renal tubular epithelial cells; IDH2, isocitrate dehydrogenase (NADP(+)) 2; ELISA, Enzyme-Linked Immunosorbent Assay; OXPHOS, oxidative phosphorylation; Co-IP, co-immunoprecipitation.

key organelles for antioxidant damage, and their dysfunction correlates with increased ROS and reduced antioxidant capacity [29]. Consistently, our research found mitochondrial dysfunction in both RIRI mice and H/R cells. Zhou *et al.* [30] reported that improving mitochondrial function alleviates kidney injury and improves renal outcomes. Our observations further indicate that enhancing mitochondrial homeostasis can counteract renal dysfunction, highlighting stable mitochondrial function as a promising therapeutic target for kidney injury.

IDH2, a mitochondrial TCA cycle enzyme, regulates production and mitochondrial homeostasis [12]. The activity of IDH2 is directly proportional to the ability of resisting oxidative stress damage in myocardial cells [31], suggesting that IDH2 has a complex regulatory mechanism in relation to cellular oxidative stress. Moreover, positive regulation of IDH2 restores mitochondrial homeostasis in renal tubular epithelial cells [32]. Our study found that increased total IDH2 and K413 acetylation levels in RIRI mouse kidneys. Simulating K413 deacetylation inhibited mtROS up-

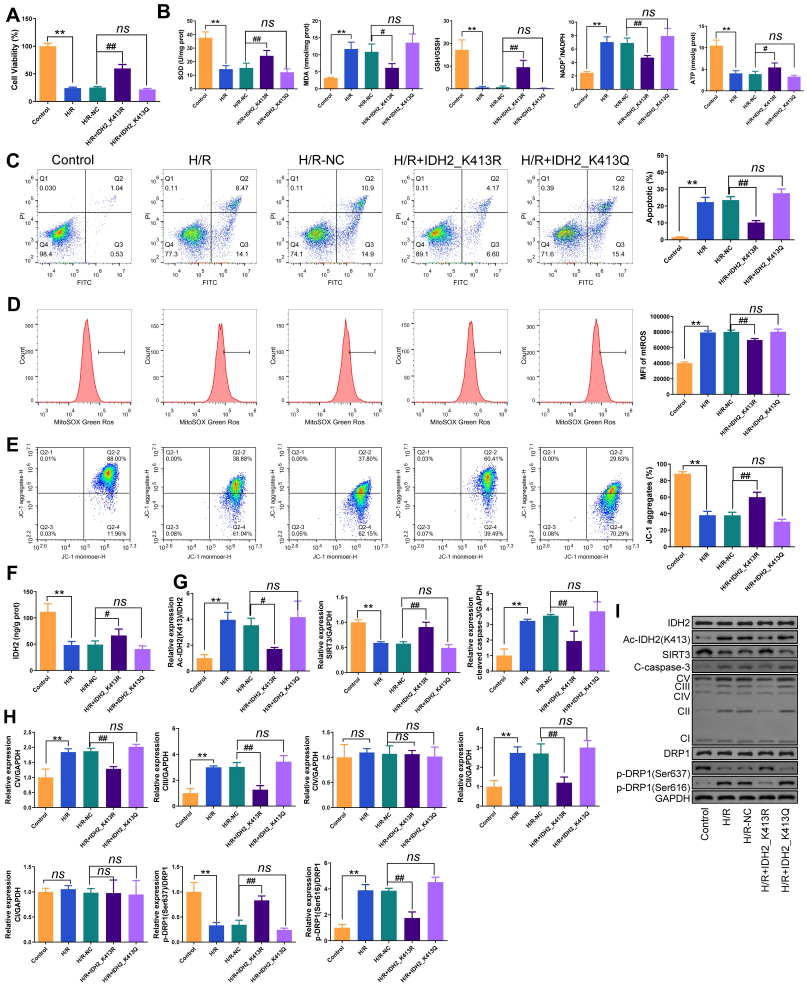

Fig. 6. Deacetylation of IDH2 improves mitochondrial function and reduces mtROS level in H/R-exposed RTECs. Directional mutation of IDH2 acetylation site (K413) was performed by transfecting with adeno-associated virus. Primarily, RTECs were cultured in a 12-h hypoxia environment followed by 24-h reoxygenation. (A) Cell counting kit 8 was used for cell viability detection. Mutating K to R (K413R) at 413-site improved RTEC viability ($n = 6$). (B) Furthermore, oxidative stress indices (MDA, SOD, and GSH/GSSG), and mitochondrial function indices ($NADP^+$/NADPH and ATP) were measured using a microplate reader. Mutating K to R (K413R) at 413-site decreased MDA, $NADP^+$/NADPH, and ATP, while increasing SOD and GSH/GSSH. (C) Annexin V-FITC/PI kit and flow cytometry were used to detect apoptosis. Mutating K to R (K413R) at 413-site decreased RTEC apoptosis. (D) MtROS were measured using a mitoSOX green fluorescence probe and flow cytometry; MFI of mtROS is the average mtROS content per mtROS-positive cell in mtROS-positive cells. Mutating K to R (K413R) at 413-site decreased mtROS in H/R-exposed RTECs with 24-h reoxygenation. (E) JC-1 staining was used to membrane potential. The membrane potential is directly proportional to the expression level of JC-1 aggregates. Mutating K to R (K413R) at 413-site increased the membrane potential of H/R-exposed RTECs. (F) IDH2 content was detected using ELISA. Mutating K to R (K413R) at 413-site increased it. (G,H) Western blot assay was used to detect protein expression in RTECs. Mutating K to R (K413R) at 413-site decreased IDH2 acetylation (K413)/IDH2, cleaved caspase-3, OXPHOS complex II/III/V (CII/CIII/CV), and p-DRP1(Ser616)/DRP1 levels in RTECs with 24-h reoxygenation, while increasing SIRT3 and p-DRP1(Ser637)/DRP1. There was no significant change in OXPHOS complex I/IV (CI/CIV) expression. (I) Representative images of protein bands. Mean ± SD, $n = 3$. $^{**}p < 0.01$, *vs.* Control group; $^{ns}p > 0.05$, $\#p < 0.05$, $\#\#p < 0.01$, vs. H/R-NC group. List of abbreviations: H/R, hypoxia/reoxygenation; RTECs, renal tubular epithelial cells; $NADP^+$, nicotinamide adenine dinucleotide phosphate; IDH2, isocitrate dehydrogenase (NADP(+)) 2; MDA, malondialdehyde; SOD, superoxide dismutase; GSH, glutathione; GSSG, glutathione disulfide; ATP, adenosine triphosphate; FITC, fluorescein isothiocyanate; Annexin V, Annexin Protein V; PI, propidium iodide; K, lysine; R, arginine; mitoSOX, mitochondrial superoxide; mtROS, mitochondrial Reactive Oxygen Species; MFI, mean fluorescence intensity; JC-1, CBIC2(3); ELISA, Enzyme-Linked Immunosorbent Assay; C-caspase-3, cleaved caspase-3; OXPHOS, oxidative phosphorylation; DRP1, dynamin-related protein 1; p-DRP1, phosphorylated DRP1; Ser, serine; GAPDH, glyceraldehyde-3-phosphate dehydrogenase.

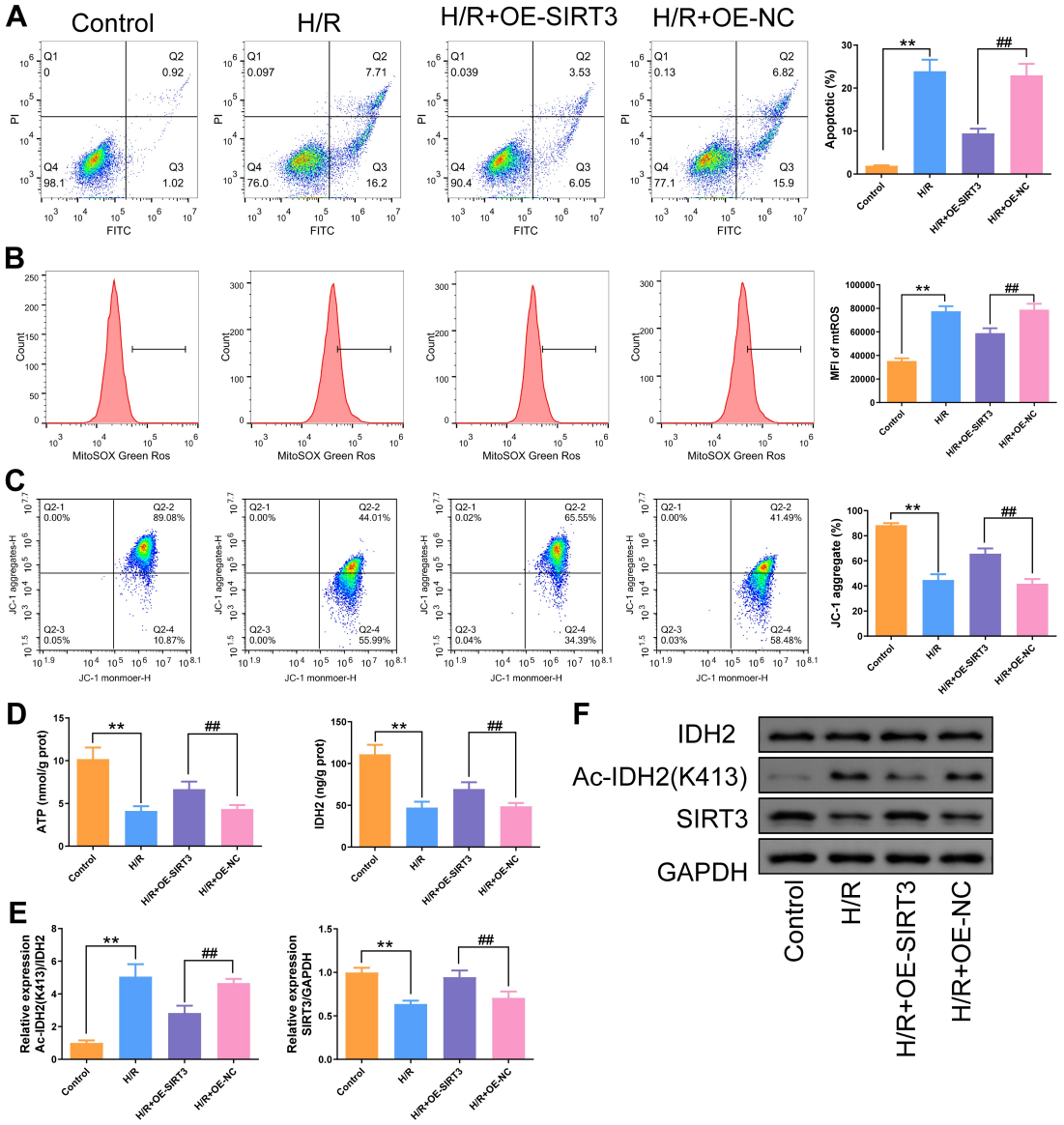

Fig. 7. Overexpression of SIRT3 inhibits apoptosis and mtROS, while improving mitochondrial dysfunction and decreasing IDH2 acetylation (K413) of H/R-exposed RTECs. Overexpressing SIRT3 was performed by plasmid transfection. Primarily, RTECs were cultured in a 12-h hypoxia environment followed by 24-h reoxygenation. (A) Annexin V-FITC/PI kit and flow cytometry were used to detect apoptosis. Overexpressing SIRT3 decreased apoptosis in H/R-exposed RTECs. (B) MtROS were measured using a mitoSOX green fluorescence probe and flow cytometry; MFI of mtROS is the average mtROS content per mtROS-positive cell in mtROS-positive cells. Overexpressing SIRT3 decreased mtROS in H/R-exposed RTECs. (C) JC-1 staining was used to membrane potential. The membrane potential is directly proportional to the expression level of JC-1 aggregates. Overexpressing SIRT3 increased the membrane potential of H/R-exposed RTECs. (D) ATP and IDH were measured using a microplate reader. Overexpressing SIRT3 increased them in H/R-exposed RTECs. (E,F) Western blot assay was used to detect protein expression in RTECs. Overexpressing SIRT3 decreased IDH2 acetylation (K413)/IDH2 while increasing SIRT3 expression. Mean ± SD, $n = 3$. $^{**}p < 0.01$, *vs.* Control group; $^{\#\#}p < 0.01$, vs. H/R-NC group. List of abbreviations: H/R, hypoxia/reoxygenation; RTECs, renal tubular epithelial cells; FITC, fluorescein isothiocyanate; Annexin V, Annexin Protein V; PI, propidium iodide; mitoSOX, mitochondrial superoxide; mtROS, mitochondrial reactive oxygen species; MFI, mean fluorescence intensity; JC-1, CBIC2(3); $NADP^+$, nicotinamide adenine dinucleotide phosphate; ATP, adenosine triphosphate; IDH2, isocitrate dehydrogenase (NADP(+)) 2; SIRT3, sirtuin 3; GAPDH, glyceraldehyde-3-phosphate dehydrogenase.

regulation, improved mitochondrial morphology, and alleviated dysfunction., highlighting K413-acetylated IDH2 as a key regulator of mitochondrial stability.

Zou *et al.* [21] reported that IDH2 acetylation promoted cellular ROS, while SIRT3 deficiency increased IDH2 acetylation. RIRI rat renal tissue exhibits SIRT3 de-

ficiency [33], and reduced SIRT3 activity correlates with lower NAD^+/NADH ratio [34]. Consistent with previous reports, we observed that H/R cells reduced SIRT3 expression, which was upregulated by IDH2 deacetylation simulation. As a NAD^+-dependent deacetylase, SIRT3 activity relates to the intracellular NAD^+ content [35]. Our data show IDH deacetylation increases renal NAD^+ and IDH activity in RTECs, promoting TCA cycle and reducing more NAD^+ to NADH. Typically, there exists a feedback mechanism for NADH oxidation-reduction to NAD^+ within cells (such as through the mitochondrial respiratory chain), which helps maintain relatively stable and sufficient levels of NAD^+ [36]. Adequate NAD^+ can provide better conditions for SIRT3 to exert its deacetylation function [34], which serve as a signal feedback to stimulate the upregulation of SIRT3 protein expression in cells [37]. Furthermore, it may promote the deacetylation of mitochondrial protein, thereby forming a synergistic mechanism based on changes in NAD^+ levels, establishing a synergistic mechanism based on alterations in NAD^+ levels, which may lead to synchronous upregulation of IDH and SIRT3 levels. Overexpressing SIRT3 in H/R cells improved mitochondrial dysfunction, increased IDH2 activity and reduced K413-acetylated IDH2 levels, confirming SIRT3 as a key regulator of IDH2 deacetylation. In summary, our research findings suggest that promoting deacetylation of IDH2 not only enhances IDH2 enzyme activity but also further promotes SIRT3 enzyme expression, with potential synergistic effects. The potential mechanism of synergistic regulation in this is worth further exploration.

Additionally, mitochondrial dysfunction is involved in the regulation of cell survival and apoptosis. Li *et al*. [38] found that fission proteins such as mitochondrial DRP1 increased in AKI animal models, which was positively correlated with the level of cell apoptosis. Improving kidney injury can inhibit cell apoptosis while reducing mitochondrial DRP1 expression, restoring mitochondrial quality and homeostasis. Given that IDH2 can regulate the expression of DRP1 in other cells [39]. We measured DRP1 protein levels in RIRI mice and H/R cells and found that there was no significant upregulation of total DRP1 in the model group. However, the phosphorylation of DRP1 at Ser637 and Ser616 showed opposite trends. Previous studies have shown that the phosphorylation of DRP1 at Ser637 inhibits the translocation of DRP1 to mitochondria and the activity of GTPase, thereby suppressing mitochondrial division, while the phosphorylation of DRP1 at Ser616 enhances the activity of DRP1, leading to mitochondrial division [40,41]. Our study suggests that the deacetylation level of IDH2 (K413) may be involved in regulating DRP1 phosphorylation, thereby reducing mitochondrial fission and maintaining mitochondrial homeostasis. It is possible that SIRT3 may target IDH2 to induce phosphorylation of Drp1 at Ser637 to block mitochondrial division, thereby antagonizing cell apoptosis.

Although we demonstrated the role of IDH2 activity in ameliorating both RIRI-induced renal injury and H/R-induced RTEC damage, and emphasized its close association with SIRT3 and IDH2 deacetylation levels, further investigations are needed. SIRT3 knockdown rescue experiments are warranted in future studies to clarify the critical role of the SIRT3-IDH2 axis in RIRI animal models and rule out the potential involvement of SIRT3's substrates. Additionally, we also found the correlation of ROS and DRP1 in RIRI model and H/R cells; ROS clearance experiments are necessary to verify their causal relationships. Moreover, it should be noted that laboratory animals and cells differ substantially from clinical settings. Further translation of these findings to clinical applications requires additional clinical data and validation across diverse animal models.

Conclusion

This study confirms that IDH2 (K413) deacetylation ameliorates RIRI-induced renal injury and H/R-induced RTEC injury. Overexpressing SIRT3 promoted IDH2 (K413) deacetylation, reduced RTEC apoptosis and improved mitochondrial dysfunction, suggesting SIRT3 improves RIRI by deacetylating IDH2 (K413). These findings shed light on AKI pathogenesis and inform therapeutic strategy.

Availability of Data and Materials

The data presented in this study are available upon request from the corresponding author.

Author Contributions

LX: Conceptualization, Formal analysis, Funding acquisition, Investigation, Project administration, Writing-original draft. BX: Data curation, Investigation, Methodology, Visualization, Writing-original draft. SY: Data curation, Investigation, Validation, Writing-review & editing. WZ: Formal analysis, Validation, Visualization, Writing-original draft. XY: Conceptualization, Formal analysis, Project administration, Supervision, Writing-review & editing. All authors read and approved the final manuscript and agreed to be accountable for all aspects of the work.

Ethics Approval and Consent to Participate

All animal experiments have been approved by Laboratory animal management and ethics committee of Zhejiang Provincial People's Hospital (Approval Number: 20230715939350) and Animal Experimentation Ethics Committee of Zhejiang Eyong Pharmaceutical Research and Development Center (Approval number: ZJEY-20230724-01).

Acknowledgment

Not applicable.

Funding

This work was supported by the Zhejiang Medicine and Health Science and Technology Project [grant number 2022494122].

Conflict of Interest

The authors declare no conflict of interest.

Supplementary Material

Supplementary material associated with this article can be found, in the online version, at https://doi.org/10.24976/Discov.Med.202638206.66.

References

[1] Ostermann M, Lumlertgul N, Jeong R, See E, Joannidis M, James M. Acute kidney injury. Lancet (London, England). 2025; 405: 241–256. https://doi.org/10.1016/S0140-6736(24)02385-7.

[2] Kellum JA, Romagnani P, Ashuntantang G, Ronco C, Zarbock A, Anders HJ. Acute kidney injury. Nature Reviews. Disease Primers. 2021; 7: 52. https://doi.org/10.1038/s41572-021-00284-z.

[3] Bauer M, Gerlach H, Vogelmann T, Preissing F, Stiefel J, Adam D. Mortality in sepsis and septic shock in Europe, North America and Australia between 2009 and 2019- results from a systematic review and meta-analysis. Critical Care (London, England). 2020; 24: 239. https://doi.org/10.1186/s13054-020-02950-2.

[4] Hou L, Wu X, Sun Z. Risk Factors and Prognosis of Acute Kidney Injury in Hospitalised Sepsis Patients. Archivos Espanoles De Urologia. 2024; 77: 263–269. https://doi.org/10.56434/j.arch.esp.urol.20247703.35.

[5] Wu QF, Kong H, Xu ZZ, Li HJ, Mu DL, Wang DX. Impact of goal-directed hemodynamic management on the incidence of acute kidney injury in patients undergoing partial nephrectomy: a pilot randomized controlled trial. BMC Anesthesiology. 2021; 21: 67. https://doi.org/10.1186/s12871-021-01288-8.

[6] Wang S, Chen Y, Han S, Liu Y, Gao J, Huang Y, *et al*. Selenium nanoparticles alleviate ischemia reperfusion injury-induced acute kidney injury by modulating GPx-1/NLRP3/Caspase-1 pathway. Theranostics. 2022; 12: 3882–3895. https://doi.org/10.7150/thno.70830.

[7] Yang M, Huang Y, Tang A, Zhang Y, Liu Y, Fan Z, *et al*. Research Hotspots in Mitochondria-Related Studies for AKI Treatment: A Bibliometric Study. Drug Design, Development and Therapy. 2024; 18: 4051–4063. https://doi.org/10.2147/DDDT.S473426.

[8] Zhao M, Wang Y, Li L, Liu S, Wang C, Yuan Y, *et al*. Mitochondrial ROS promote mitochondrial dysfunction and inflammation in ischemic acute kidney injury by disrupting TFAM-mediated mtDNA maintenance. Theranostics. 2021; 11: 1845–1863. https://doi.org/10.7150/thno.50905.

[9] Zhang X, Agborbesong E, Li X. The Role of Mitochondria in Acute Kidney Injury and Chronic Kidney Disease and Its Therapeutic Potential. International Journal of Molecular Sciences. 2021; 22: 11253. https://doi.org/10.3390/ijms222011253.

[10] Chang LY, Chao YL, Chiu CC, Chen PL, Lin HYH. Mitochondrial Signaling, the Mechanisms of AKI-to-CKD Transition and Potential Treatment Targets. International Journal of Molecular Sciences. 2024; 25: 1518. https://doi.org/10.3390/ijms25031518.

[11] Yu H, Jin F, Liu D, Shu G, Wang X, Qi J, *et al*. ROS-responsive nano-drug delivery system combining mitochondria-targeting ceria nanoparticles with atorvastatin for acute kidney injury. Theranostics. 2020; 10: 2342–2357. https://doi.org/10.7150/thno.40395.

[12] Ivanov S, Nano O, Hana C, Bonano-Rios A, Hussein A. Molecular Targeting of the Isocitrate Dehydrogenase Pathway and the Implications for Cancer Therapy. International Journal of Molecular Sciences. 2024; 25: 7337. https://doi.org/10.3390/ijms25137337.

[13] Li JJ, Yu T, Zeng P, Tian J, Liu P, Qiao S, *et al*. Wild-type IDH2 is a therapeutic target for triple-negative breast cancer. Nature Communications. 2024; 15: 3445. https://doi.org/10.1038/s41467-024-47536-6.

[14] Corridon PR. Enhancing the expression of a key mitochondrial enzyme at the inception of ischemia-reperfusion injury can boost recovery and halt the progression of acute kidney injury. Frontiers in Physiology. 2023; 14: 1024238. https://doi.org/10.3389/fphys.2023.1024238.

[15] Zheng D, Qiwen Zeng, He D, He Y, Yang J. SIRT5 alleviates hepatic ischemia and reperfusion injury by diminishing oxidative stress and inflammation via elevating SOD1 and IDH2 expression. Experimental Cell Research. 2022; 419: 113319. https://doi.org/10.1016/j.yexcr.2022.113319.

[16] Kolb AL, Corridon PR, Zhang S, Xu W, Witzmann FA, Collett JA, *et al*. Exogenous Gene Transmission of Isocitrate Dehydrogenase 2 Mimics Ischemic Preconditioning Protection. Journal of the American Society of Nephrology: JASN. 2018; 29: 1154–1164. https://doi.org/10.1681/ASN.2017060675.

[17] Fu Z, Kim H, Morse PT, Lu MJ, Hüttemann M, Cambronne XA, *et al*. The mitochondrial NAD^+ transporter SLC25A51 is a fasting-induced gene affecting SIRT3 functions. Metabolism: Clinical and Experimental. 2022; 135: 155275. https://doi.org/10.1016/j.metabol.2022.155275.

[18] Yuan J, Zhao J, Qin Y, Zhang Y, Wang A, Ma R, *et al*. The protective mechanism of SIRT3 and potential therapy in acute kidney injury. QJM: Monthly Journal of the Association of Physicians. 2024; 117: 247–255. https://doi.org/10.1093/qjmed/hcad152.

[19] Zhu M, He J, Xu Y, Zuo Y, Zhou W, Yue Z, *et al*. AMPK activation coupling SENP1-Sirt3 axis protects against acute kidney injury. Molecular Therapy: the Journal of the American Society of Gene Therapy. 2023; 31: 3052–3066. https://doi.org/10.1016/j.ymthe.2023.08.014.

[20] Juszczak F, Arnould T, Declèves AE. The Role of Mitochondrial Sirtuins (SIRT3, SIRT4 and SIRT5) in Renal Cell Metabolism: Implication for Kidney Diseases. International Journal of Molecular Sciences. 2024; 25: 6936. https://doi.org/10.3390/ijms25136936.

[21] Zou X, Zhu Y, Park SH, Liu G, O'Brien J, Jiang H, *et al*. SIRT3-Mediated Dimerization of IDH2 Directs Cancer Cell Metabolism and Tumor Growth. Cancer Research. 2017; 77: 3990–3999. https://doi.org/10.1158/0008-5472.CAN-16-2393.

[22] Smolková K, Špačková J, Gotvaldová K, Dvořák A, Křenková A, Hubálek M, *et al*. SIRT3 and GCN5L regulation of NADP+- and NADPH-driven reactions of mitochondrial isocitrate dehydrogenase IDH2. Scientific Reports. 2020; 10: 8677. https://doi.org/10.1038/s41598-020-65351-z.

[23] Chen D, Xia S, Zhang R, Li Y, Famulare CA, Fan H, *et al*. Lysine acetylation restricts mutant IDH2 activity to optimize transformation in AML cells. Molecular Cell. 2021; 81: 3833–3847.e11. https://doi.org/10.1016/j.molcel.2021.06.027.

[24] Ma LL, Kong FJ, Ma YJ, Guo JJ, Wang SJ, Dong Z, *et al*. Hypertrophic preconditioning attenuates post-myocardial infarction injury through deacetylation of isocitrate dehydrogenase 2. Acta Pharmacologica Sinica. 2021; 42: 2004–2015. https://doi.org/10.1038/s41401-021-00699-0.

[25] Devarapu SK, Grill JF, Xie J, Weidenbusch M, Honarpisheh M, Vielhauer V, *et al*. Tumor necrosis factor superfamily ligand mRNA expression profiles differ between humans and mice during homeostasis and between various murine kidney injuries. Journal of Biomedical Science. 2017; 24: 77. https://doi.org/10.1186/s12929-017-0383-3.

[26] He Y, Lang X, Cheng D, Zhang T, Yang Z, Xiong R. miR 30a 5p inhibits hypoxia/reoxygenation induced oxidative stress and apoptosis in HK 2 renal tubular epithelial cells by targeting glutamate dehydrogenase 1 (GLUD1). Oncology Reports. 2020; 44: 1539–1549. https://doi.org/10.3892/or.2020.7718.

[27] Godoy JR, Watson G, Raspante C, Illanes O. An Effective Mouse Model of Unilateral Renal Ischemia-Reperfusion Injury. Journal of Visualized Experiments: JoVE. 2021; 10.3791/62749. https://doi.org/10.3791/62749.

[28] De Silva PMCS, Gunasekara TDKSC, Gunarathna SD, Sandamini PMMA, Pinipa RAI, Ekanayake EMDV, *et al*. Urinary Biomarkers of Renal Injury KIM-1 and NGAL: Reference Intervals for Healthy Pediatric Population in Sri Lanka. Children (Basel, Switzerland). 2021; 8: 684. https://doi.org/10.3390/children8080684.

[29] Bhatti JS, Bhatti GK, Reddy PH. Mitochondrial dysfunction and oxidative stress in metabolic disorders - A step towards mitochondria based therapeutic strategies. Biochimica et Biophysica Acta. Molecular Basis of Disease. 2017; 1863: 1066–1077. https://doi.org/10.1016/j.bbadis.2016.11.010.

[30] Zhou X, Fu X, Meng YW, Dai P, Jiang Q, Yin HH, *et al*. Targeting CDC42 Protects Mitochondrial Function through KLF2/HIF-1α/PINK1 Signaling in Acute Kidney Injury. International Journal of Biological Sciences. 2026; 22: 1247–1265. https://doi.org/10.7150/ijbs.125930.

[31] ElBeck Z, Hossain MB, Siga H, Oskolkov N, Karlsson F, Lindgren J, *et al*. Epigenetic modulators link mitochondrial redox homeostasis to cardiac function in a sex-dependent manner. Nature Communications. 2024; 15: 2358. https://doi.org/10.1038/s41467-024-46384-8.

[32] Liu X, Zhang Y, Wang Y, Yang Y, Qiao Z, Zhan P, *et al*. Tubular MYDGF Slows Progression of Chronic Kidney Disease by Maintaining Mitochondrial Homeostasis. Advanced Science (Weinheim, Baden-Wurttemberg, Germany). 2025; 12: e2409756. https://doi.org/10.1002/advs.202409756.

[33] Peerapanyasut W, Kobroob A, Palee S, Chattipakorn N, Wongmekiat O. Bisphenol A aggravates renal ischemia-reperfusion injury by disrupting mitochondrial homeostasis and N-acetylcysteine mitigates the injurious outcomes. IUBMB Life. 2020; 72: 758–770. https://doi.org/10.1002/iub.2175.

[34] Ogura Y, Kitada M, Xu J, Monno I, Koya D. CD38 inhibition by apigenin ameliorates mitochondrial oxidative stress through restoration of the intracellular NAD^+/NADH ratio and Sirt3 activity in renal tubular cells in diabetic rats. Aging. 2020; 12: 11325–11336. https://doi.org/10.18632/aging.103410.

[35] Klimova N, Fearnow A, Long A, Kristian T. NAD^+ precursor modulates post-ischemic mitochondrial fragmentation and reactive oxygen species generation via SIRT3 dependent mechanisms. Experimental Neurology. 2020; 325: 113144. https://doi.org/10.1016/j.expneurol.2019.113144.

[36] Anderson KA, Madsen AS, Olsen CA, Hirschey MD. Metabolic control by sirtuins and other enzymes that sense NAD^+, NADH, or their ratio. Biochimica et Biophysica Acta. Bioenergetics. 2017; 1858: 991–998. https://doi.org/10.1016/j.bbabio.2017.09.005.

[37] Sun C, Xiong H, Guo T. β-Nicotinamide Mononucleotide Alleviates Sepsis-associated Acute Kidney Injury by Activating NAD^+/SIRT3 Signaling. Cell Biochemistry and Biophysics. 2024; 83: 2089–2099. https://doi.org/10.1007/s12013-024-01619-9.

[38] Li H, Leung JCK, Yiu WH, Chan LYY, Li B, Lok SWY, *et al*. Tubular β-catenin alleviates mitochondrial dysfunction and cell death in acute kidney injury. Cell Death & Disease. 2022; 13: 1061. https://doi.org/10.1038/s41419-022-05395-3.

[39] Park JB, Nagar H, Choi S, Jung SB, Kim HW, Kang SK, *et al*. IDH2 deficiency impairs mitochondrial function in endothelial cells and endothelium-dependent vasomotor function. Free Radical Biology & Medicine. 2016; 94: 36–46. https://doi.org/10.1016/j.freeradbiomed.2016.02.017.

[40] Chen L, Chen XY, Wang QL, Yang SJ, Zhou H, Ding LS, *et al*. Astragaloside IV Derivative (LS-102) Alleviated Myocardial Ischemia Reperfusion Injury by Inhibiting Drp1^{Ser616} Phosphorylation-Mediated Mitochondrial Fission. Frontiers in Pharmacology. 2020; 11: 1083. https://doi.org/10.3389/fphar.2020.01083.

[41] Wu NS, Ma IC, Lin YF, Ko HJ, Loh JK, Hong YR. The mystery of phospho-Drp1 with four adaptors in cell cycle: when mitochondrial fission couples to cell fate decisions. Cell Cycle (Georgetown, Tex.). 2023; 22: 2485–2503. https://doi.org/10.1080/15384101.2023.2289753.